

1 **UV and Infrared Absorption Spectra, Atmospheric Lifetimes, and Ozone Depletion and**
2 **Global Warming Potentials for CCl₂FCCl₂F (CFC-112), CCl₃CClF₂ (CFC-112a), CCl₃CF₃**
3 **(CFC-113a), and CCl₂FCF₃ (CFC-114a)**

4 Maxine E. Davis,^{1,2,3} François Bernard,^{1,2} Max R. McGillen,^{1,2}
5 Eric L. Fleming,^{4,5} and James B. Burkholder¹

6 ¹ Earth System Research Laboratory, Chemical Sciences Division, National Oceanic and
7 Atmospheric Administration, Boulder, Colorado, USA.

8 ² Cooperative Institute for Research in Environmental Sciences, University of Colorado,
9 Boulder, Colorado, USA.

10 ³ Michigan State University, Lyman Briggs College, East Lansing, MI.

11 ⁴ NASA Goddard Space Flight Center, Greenbelt, Maryland, USA.

12 ⁵ Science Systems and Applications, Inc., Lanham, Maryland, USA.

13
14
15
16 Corresponding author: James B. Burkholder, NOAA, 325 Broadway, Boulder, CO 80305, USA.
17 (James.B.Burkholder@noaa.gov)

23 **Abstract** The potential impact of CCl_2FCF_3 (CFC-114a) and the recently observed $\text{CCl}_2\text{FCCl}_2\text{F}$
24 (CFC-112), $\text{CCl}_3\text{CClF}_2$ (CFC-112a), and CCl_3CF_3 (CFC-113a) and ~~CCl_2FCF_3 (CFC-114a)~~
25 chlorofluorocarbons (CFCs), on stratospheric ozone and climate are presently not well
26 characterized. In this study, the UV absorption spectra of these CFCs were measured between
27 192.5–235 nm over the temperature range 207–323 K. Precise parameterizations of the UV
28 absorption spectra are presented. A 2-D atmospheric model was used to evaluate the CFC
29 atmospheric loss processes, lifetimes, ozone depletion potentials (ODPs), and the associated
30 uncertainty ranges in these metrics due to the kinetic and photochemical uncertainty. The CFCs
31 are primarily removed in the stratosphere by short wavelength UV photolysis with calculated
32 global annually averaged steady-state lifetimes (years) of 63.6 (61.9–64.7), 51.5 (50.0–52.6),
33 55.4 (54.3–56.3), and 105.3 (102.9–107.4) for CFC-112, CFC-112a, CFC-113a, and CFC-114a,
34 respectively. The range of lifetimes given in parentheses are due to where obtained by including
35 the 2σ uncertainty in the UV absorption spectra and $\text{O}(^1\text{D})$ rate coefficients included in the
36 model calculations. The 2-D model was also used to calculate the CFC ozone depletion
37 potentials (ODPs) with values of 0.98, 0.86, 0.73, and 0.72 obtained for CFC-112, CFC-112a,
38 CFC-113a, and CFC-114a, respectively. Using the infrared absorption spectra and lifetimes
39 determined in this work, the CFCs global warming potentials (GWPs) were estimated to be 4260
40 (CFC-112), 3330 (CFC-112a), 3650 (CFC-113a), and 6510 (CFC-114a) for the 100-year time-
41 horizon.

42
43
44

45 1. Introduction

46 Chlorofluorocarbons (CFCs) are potent ozone depleting and greenhouse gases that were
47 phased-out of production under the Montreal Protocol Agreement (1987) and its subsequent
48 amendments and adjustments. Laube et al. (2014) recently reported the first observation of
49 tetrachloro-1,2-difluoroethane ($\text{CCl}_2\text{FCCl}_2\text{F}$, CFC-112), tetrachloro-1,1-difluoroethane
50 ($\text{CCl}_3\text{CClF}_2$, CFC-112a), and 1,1,1-trichloro-2,2,2-trifluoroethane (CCl_3CF_3 , CFC-113a) in the
51 atmosphere with emission sources dating back to the 1960s. The atmospheric **mixing ratios**
52 **loading** in the year 2000 were found to be ~ 0.5 ppt (**parts per trillion**) (CFC-112), ~ 0.08 ppt
53 (CFC-112a), and ~ 0.3 ppt (CFC-113a), which are minor compared to a total chlorine **loading**
54 **mixing ratio** of 3.3 ppb (**parts per billion**) (year 2012), where CCl_3F (CFC-11), CCl_2F_2 (CFC-12),
55 and $\text{CCl}_2\text{FCClF}_2$ (CFC-113) account for $\sim 60\%$ of the total (WMO, 2014). The atmospheric
56 **abundance mixing ratio** of CFC-112 and CFC-112a was found to have leveled off in the late
57 1990's, while the **abundance mixing ratio** of CFC-113a was found to be increasing through to the
58 present day, which is contrary to the objectives of the Montreal Protocol. Laube et al. (2014)
59 estimated the stratospheric lifetimes for these substances, using a tracer-tracer analysis, to be 51
60 (37–82), 44 (28–98), and 51 (27–264) years for CFC-112, CFC-112a, and CFC-113a,
61 respectively, where the values in parentheses are the range of the lifetimes determined in their
62 analysis. The inferred ozone depletion potentials (ODPs) were 0.88 (0.62–1.44), 0.88 (0.5–
63 2.19), and 0.68 (0.34–3.79) for CFC-112, CFC-112a, and CFC-113a, respectively, where the
64 range in parentheses was derived from the range in the CFC lifetime given above. **Atmospheric**
65 **measurements of CFC-114 are estimated to include a $\sim 10\%$ fraction due to CFC-114a (WMO,**
66 **2014). The atmospheric lifetime of CFC-114a is estimated to be similar to that of CFC-12, i.e.,**
67 **~ 100 years (WMO, 2014).** It is clear that the CFCs are long-lived compounds and potent ozone
68 depleting substances and greenhouse gases. It is expected that these compounds would be
69 predominantly removed from the atmosphere via short wavelength UV photolysis, primarily in
70 the stratosphere. However, to date, there are no UV absorption spectra for these compounds
71 available, which are needed to better evaluate their atmospheric impact.

72 In this study, UV absorption spectra were measured for CFC-112, CFC-112a, CFC-113a,
73 and 1,1-dichlorotetrafluoroethane (CCl_2FCF_3 , CFC-114a) between 192.5 and 235 nm over the
74 temperature range 207–323 K. The Goddard Space Flight Center (GSFC) 2-D atmospheric
75 model was used to evaluate the reactive and photolytic loss processes and calculate globally

76 averaged lifetimes and ozone depletion potentials. In addition, infrared absorption spectra were
77 measured at 296 K for these compounds and used to estimate their global warming potentials
78 (GWPs). The present results are compared with results from the previous infrared studies of
79 Olliff and Fischer (1992; 1994) (CFCs 112, 112a, 113a, and 114a) and Etminan et al. (2014)
80 (CFC-113a) where possible.

81 2. Experimental Details

82 2.1 UV Measurements

83 The experimental apparatus has been described in detail previously (McGillen et al.,
84 2013; Papadimitriou et al., 2013a; 2013b) and is only briefly discussed here. The output of a
85 stable 30 W deuterium (D₂) lamp light source was collimated and directed through a jacketed
86 90.4 ± 0.3 cm single pass absorption cell. The beam exiting the cell was focused onto the
87 entrance slit (150 μm) of a 0.25 m monochromator (~1 nm resolution) and detected using a
88 photomultiplier tube (PMT). The temperature of the absorption cell was controlled to within ±1
89 K. Absorption measurements were made at 10 discrete wavelengths at temperatures between
90 207 and 323 K to enable spectrum parameterizations appropriate for stratospheric conditions.

91 Beer's law was applied to determine the absorption cross section, $\sigma(\lambda, T)$, at each
92 wavelength and temperature:

$$93 \quad A(\lambda, T) = \ln \left[\frac{I_0(\lambda) - I_d}{I(\lambda) - I_d} \right] = \sigma(\lambda, T) \times L \times [\text{CFC}] \quad (1)$$

94 where $A(\lambda, T)$ is the absorbance at wavelength λ and temperature T , I_d is the signal recorded in
95 the absence of light, $I_0(\lambda)$ and $I(\lambda)$ are the measured signal in the absence and presence of the
96 CFC sample, L is the cell pathlength, and $[\text{CFC}]$ is the gas-phase CFC concentration. The PMT
97 signal was recorded with a 1 kHz sampling rate and a ~20 s average was used in the data
98 analysis. $I_0(\lambda)$ was recorded at the beginning and end of each measurement, which typically
99 agreed to 0.1%, or better. Absorbance measurements were made at each wavelength over a
100 range of CFC concentration under static conditions. The CFCs were added to the absorption cell
101 from dilute mixtures and the CFC concentration was determined using the sample mixing ratio,
102 the absorption cell pressure and temperature, and the ideal gas law. A linear least-squares fit of
103 $A(\lambda, T)$ versus $[\text{CFC}]$ was used to obtain $\sigma(\lambda, T)$.

104 For the CFC-112 and CFC-112a measurements, an optical neutral density filter was
105 inserted between the D₂ lamp and the absorption cell to attenuate the probe beam and minimize

106 CFC loss due to photolysis (sample photolysis was not observed for CFC-113a and CFC-114a).
107 In addition, a mechanical shutter blocked the D₂ lamp beam while the absorption cell was being
108 filled. Under most conditions, photolytic loss of the CFC-112 and CFC-112a was undetectable.
109 However, at the higher concentrations used in this study minor photolytic loss (<2%) was
110 observed. In these cases, a least-squares fit of the first ~20 s of the PMT signal was used in the
111 data analysis to obtain the initial $I(\lambda)$ signal.

112 2.2 Infrared Absorption Measurements

113 Infrared absorption spectra at 296 K for CFC-112, CFC-112a, CFC-113a, and CFC-114a
114 were measured over the 500 to 4000 cm⁻¹ wavenumber range using Fourier transform infrared
115 (FTIR) spectroscopy. Measurements were made using a 15 cm single pass Pyrex absorption cell
116 and a MCT detector at a resolution of 1 cm⁻¹ with 100 co-adds. The CFC sample was introduced
117 into the absorption cell from a dilute mixture prepared off-line and the CFC concentration was
118 determined using the ideal gas law. Absorption cross sections were determined using Beer's
119 law, equation 1, with the spectrum measurements consisting of ~10 different concentrations.
120 The concentration ranges used were (in 10¹⁶ molecule cm⁻³): (0.348–10.2), (0.453–3.84), (0.376–
121 1.90), and (0.279–4.02) for CFC-112, CFC-112a, CFC-113a, and CFC-114a, respectively. The
122 infrared absorption spectra recorded for CFC-112 and CFC-112a were corrected for the presence
123 of a minor (~4%) isomer impurity as determined from a ¹⁹F NMR sample analysis.

124 2.3 Materials

125 Samples of CCl₂FCCL₂F (CFC-112, 97% stated purity), CCl₃CClF₂ (CFC-112a, 96%
126 stated purity), CCl₃CF₃ (CFC-113a, 99% stated purity), and CCl₂FCF₃ (CFC-114a, 99.9% stated
127 purity) were obtained commercially. The samples were processed in several freeze (77 K)-
128 pump-thaw cycles prior to use. The CFC-114a sample was also treated with freeze (197 K)-
129 pump-thaw cycles to remove CO₂ from the sample. The liquid CFC-112, CFC-112a, and CFC-
130 113a samples were stored under vacuum in Pyrex reservoirs. The CFC-112 and CFC-112a
131 samples contained minor isomeric impurities, which were quantified using ¹⁹F NMR to be
132 0.960/0.040 (CFC-112a/CFC-112) for the CFC-112a sample and 0.963/0.0368 (CFC-112/CFC-
133 112a) for the CFC-112 sample. Dilute mixtures of the CFCs in a He (UHP, 99.999%) bath gas
134 were prepared manometrically in 12 L Pyrex bulbs and used to deliver the CFC sample to the
135 UV and infrared absorption cells. Over the course of the study, multiple gas mixtures were
136 prepared for each of the CFCs with mixing ratios ranging between 0.5 and 27%. The dilute

137 mixtures were prepared with an estimated accuracy of $\pm\sim 1\%$. The UV and infrared spectra
138 obtained for the CFCs were independent of the sample mixing ratio and absorption cell total
139 pressure. Pressures were measured using calibrated capacitance manometers. Uncertainties
140 given throughout the paper are 2σ unless noted otherwise.

141 3. Results and Discussion

142 The absorption spectrum, $\sigma(\lambda, T)$, measurements obeyed Beer's law with fit precisions of
143 $\sim 1\%$, or less, for all wavelengths and temperatures included in this study. Replicate
144 measurements using different sample mixing ratios, bath gas, range of absorption, and optical
145 filtering agreed to within the measurement precision and were combined in a global linear least-
146 squares fit in the final data analysis.

147 The UV absorption spectra of the CFC-112 and CFC-112a samples were measured at 10
148 discrete wavelengths between 192.5 nm and 235 nm at 5 discrete temperatures between 230 and
149 323 K. The results, not corrected for the isomeric impurity present in the samples, are
150 summarized in Tables S1 and S2 and shown in Figures S1 and S2 of the Supporting Information.
151 To account for the isomeric impurity, $\sigma(\lambda, T)$ for CFC-112 and CFC-112a were parameterized
152 using the empirical formula:

$$153 \ln(\sigma(\lambda, T)) = \sum_i A_i \lambda_i^i + (T - 296) \sum_i B_i \lambda_i^i \quad (2)$$

154 The parameterizations reproduced the experimental data to better than $\sim 2\%$ over the wavelength
155 range most critical to atmospheric photolysis, i.e., between 195 and 215 nm. The results from
156 the ^{19}F NMR sample analysis were then used to obtain the final spectrum parameterizations.

157 The UV absorption spectra for CFC-113a and CFC-114a were measured at 10 discrete
158 wavelengths between 192.5 and 235 nm at 6 discrete temperatures between 207 and 323 K. The
159 cross section results are given in Tables 1 and 2 and shown in Figures 1 and 2. The CFC UV
160 absorption spectra were parameterized using equation 2. The parameterizations reproduced the
161 experimental data to within $\sim 4\%$, or better, as shown in Figures 1 and 2.

162 The fit parameters are given in Table 3 and a comparison of the parameterized 296 K
163 spectra is shown in Figure 3. The UV absorption spectra of the CFCs are continuous over the
164 wavelength range included in this study with a precipitous decrease in cross section with
165 increasing wavelength. A decrease in $\sigma(\lambda, T)$ with decreasing temperature was observed at
166 nearly all wavelengths included in this study with the temperature dependence being greatest at

167 the longer wavelengths, see Figures 1, 2, and S1 and S2. The inclusion of the $\sigma(\lambda, 323 \text{ K})$
168 measurements, although not entirely atmospherically relevant, was included in the study to better
169 define the absorption spectrum temperature dependence and its parameterization. As shown in
170 Figure 3, the UV absorption spectra for the CFCs show distinct differences in their absolute cross
171 sections and wavelength dependence over the region most critical for determining their
172 atmospheric photolysis rates, i.e., lifetimes. The spectra demonstrate that CFCs with increased
173 chlorine content are stronger absorbers in this wavelength region, although the molecular
174 structure of the molecule also plays an important role. For example, the $\text{C}_2\text{Cl}_4\text{F}_2$ isomer with
175 more chlorine atoms on a carbon atom, CFC-112a ($\text{CCl}_3\text{CClF}_2$), absorbs more strongly than
176 CFC-112 ($\text{CCl}_2\text{FCCl}_2\text{F}$).

177 The spectrum parameterizations given in Table 3 reproduce the experimental data very
178 well. The overall 2σ uncertainty in $\sigma(\lambda, T)$ for CFC-112, CFC-112a, CFC-113, and CFC-114a,
179 including estimated systematic errors, is estimated to be $\sim 4\%$ over the range of wavelengths and
180 temperatures included in this study.

181 The measured infrared spectra for each of the CFCs obeyed Beer's law with a fit
182 precision of $\sim 0.3\%$ and were independent of total pressure over the pressure range 20–250 Torr
183 (He bath gas). The infrared spectra are shown in Figure 4 and digitized spectra are available in
184 the Supporting Information. Table S3 in the Supporting Information provides a detailed
185 comparison of our results with those of Olliff and Fischer (1992; 1994) for all the CFCs and
186 Etminan et al. (2014) for CFC-113a. Overall the agreement between the studies is better than
187 10%.

188 **4. Atmospheric Implications**

189 The atmospheric loss processes, lifetimes, ODPs, and associated uncertainties for the
190 CFCs included in this study were quantified using the Goddard Space Flight Center (GSFC) 2-D
191 atmospheric model (Fleming et al., 2011). The calculations used the UV spectrum
192 parameterizations obtained in this work with an assumed unit photolysis quantum yield at all
193 wavelengths. As discussed in section 3, an overall 2σ uncertainty of 4% was used at all
194 wavelengths and temperatures for the UV cross sections of the four CFCs. For Lyman-
195 α (121.567 nm), absorption cross sections are not available for these CFCs and values (in units
196 of $10^{-17} \text{ cm}^2 \text{ molecule}^{-1}$) of 13, 15, 9.8, and 2 were estimated for CFC-112, CFC-112a, CFC-

197 113a, and CFC-114a, respectively, based on values available for similar molecules (see Ko et al.
 198 (2013), Chapter 3). An estimated Lyman- α cross section uncertainty factor of 2 (2σ) was used.
 199 Rate coefficients for the O(¹D) reaction with CFC-113a and CFC-114a were taken from
 200 Baasandorj et al. (2011) with 2σ uncertainty factors of 1.25 and 1.2, respectively (Burkholder et
 201 al., 2015b). Rate coefficients for the O(¹D) reaction with CFC-112 and CFC-112a were
 202 estimated to be $3 \times 10^{-10} \text{ cm}^3 \text{ molecule}^{-1} \text{ s}^{-1}$ with a 0.9 reactive branching ratio and an uncertainty
 203 factor of 1.5 (2σ). All other kinetic and photochemical parameters were taken from Sander et al.
 204 (2011). All model results presented in this study are for year 2010 ~~2000~~ steady-state conditions.
 205 Surface mixing ratio boundary conditions for 2010 are based on the Laube et al. (2014) results
 206 for CFC-112, CFC-112a, and CFC-113a; for CFC-114a, a 2010 value of 1.6 ppt is used, based
 207 on measurements of CFC-114 which are a combination of CFC-114 and CFC-114a, with an
 208 assumed relative contribution of 10% for CFC-114a (WMO, 2014).

209 Model calculations of the CFC fractional atmospheric loss processes are given in Table 4
 210 and the altitude profiles for CFC-112 are shown in Figure 5. The calculated atmospheric profiles
 211 for CFC-112a, CFC-113a, and CFC-114a are provided in the Supporting Information. UV
 212 photolysis is the predominant atmospheric loss process for each of the CFCs. Lyman- α
 213 photolysis is important only in the mesosphere above 65 km; it has a negligible contribution to
 214 the overall global loss (<0.001). The O(¹D) reaction is a minor stratospheric loss process, $\sim 2\%$,
 215 for CFC-112, CFC-112, and CFC-113a, but more significant for CFC-114a, $\sim 7\%$. The UV
 216 photolysis and O(¹D) reactive loss of the CFCs leads to the direct release of reactive chlorine and
 217 the formation of chlorine containing radicals (Burkholder et al., 2015a).

218 The CFC lifetimes were computed as the ratio of the annually averaged global
 219 atmospheric burden to the vertically integrated annually averaged total global loss rate (Ko et al.,
 220 2013). The total global lifetime (τ_{Tot}) was also separated by the troposphere (τ_{Trop} , surface to the
 221 tropopause, seasonally and latitude-dependent), stratosphere (τ_{Strat}), and mesosphere (τ_{Meso} , <1
 222 hPa) using the total global atmospheric burden and the loss rate integrated over the different
 223 atmospheric regions such that

$$224 \quad \frac{1}{\tau_{\text{Tot}}} = \frac{1}{\tau_{\text{Trop}}} + \frac{1}{\tau_{\text{Strat}}} + \frac{1}{\tau_{\text{Meso}}} \quad (2)$$

225 The 2-D model total global annually averaged lifetimes and the range in lifetimes are given in
 226 Table 5. The 2σ range in the lifetime was calculated using the absolute 2σ maximum and

227 minimum in the UV absorption spectra and estimated Lyman- α cross sections reported in the
228 present work, along with the 2σ uncertainties in the O(¹D) rate coefficients taken from Sander et
229 al. (2011). The CFCs are long-lived and primarily removed in the stratosphere by UV
230 photolysis. The uncertainty in the calculated lifetime due to the uncertainty in the UV absorption
231 spectra measured in this work is small, <2%. The absolute lifetime uncertainty due to the kinetic
232 and photochemical input parameters is expected to be small compared to that calculated using
233 different atmospheric models due to the individual model treatment of dynamics, chemistry,
234 radiation, numerics, and other processes (Chipperfield et al., 2014; Ko et al., 2013). **In general,**
235 **the lifetime uncertainty due to the kinetic and photochemical input parameters is also expected to**
236 **be small compared to the uncertainty due to transport processes and actinic fluxes (due to, for**
237 **example, uncertainty in the J[O₂] cross sections; e.g., see Ko et al. (2013)). However, evaluation**
238 **of all processes that contribute to uncertainty in the total CFC lifetime is beyond the scope of the**
239 **present paper.**

240 The model calculated stratospheric lifetimes for CFC-112, CFC-112a, and CFC-113a are
241 in reasonable agreement with the values of 51 (37–82), 44 (28–98), and 51 (27–264) years
242 reported by Laube et al. (2014) (uncertainty ranges in parentheses). The lifetimes reported by
243 Laube et al. were based on a tracer-tracer analysis (see Plumb and Ko (1992) and Volk et al.
244 (1997) for method details) using a reference CFC-11 lifetime of 45 years. Scaling to the 52 year
245 CFC-11 lifetime given in WMO (2014) brings the results into better agreement with the present
246 work. The range of lifetimes obtained in the model results, which was determined solely based
247 on the uncertainty in the kinetic and photochemical input parameters, is, however, significantly
248 less than obtained in the tracer-tracer analysis. It is worth noting that while the total global
249 lifetimes of the isomers CFC-112 and CFC-112a are similar, the lifetimes of CFC-113a (55.4
250 yrs) and CFC-114a (105.3 yrs) are substantially shorter (by ~60%) than those of the isomers
251 CFC-113 (93 yrs) and CFC-114 (189 yrs) (WMO, 2014).

252 **4.1. Ozone Depletion Potentials (ODPs)**

253 The semi-empirical and model calculated ODPs for the CFCs are given in Table 6. The
254 ODP was calculated following the methodology used previously (Fisher et al., 1990; Wuebbles,
255 1983). Steady-state simulations for year **2010** ~~2000~~ were run with the surface boundary
256 conditions for the four CFCs and CFC-11 (used as the reference compound) increased
257 individually to obtain a ~1% depletion in annually averaged global total ozone. The ODP was

258 then taken as the change in global ozone per unit mass emission of the CFC relative to the
259 change in global ozone per unit mass emission of CFC-11. Each of these compounds is a potent
260 ozone depleting substance. The model calculated ODPs for CFC-112, CFC-112a, and CFC-113a
261 are similar to the semi-empirical values inferred by Laube et al. (2014). The **small** range
262 ($\leq \pm 0.015$) in the model ODP values **is primarily** due to **the relatively small** uncertainty in the UV
263 spectra obtained in this work **was found to be small** ($\leq \pm 0.015$).

264 Table 6 also includes ODPs for CFC-113 and CFC-114. These are larger than the ODPs
265 for the isomers CFC-113a and CFC-114a (especially CFC-113 vs CFC-113a), likely due in part,
266 to the longer lifetimes of CFC-113 and CFC-114. For comparison with other related compounds,
267 the ODPs of CFC-115, CFC-12, and CCl_4 are also included in Table 6. This shows the general
268 decrease in ODP with decreasing chlorination among CFC-112a, CFC-112, CFC-113a, CFC-
269 113, CFC-114a, CFC-114, and CFC-115. We also note that the model ODPs for CFC-112 and
270 CFC-112a are generally similar, although slightly less, than CCl_4 which also contains 4 chlorine
271 atoms. For most of the compounds listed in Table 6, the model ODPs are larger than the semi-
272 empirical values. **The semi-empirical ODPs are dependent on observationally-based fractional**
273 **release factors for a given stratospheric mean age of air, i.e., the fractional amount of a CFC that**
274 **has been dissociated at a given point in the stratosphere (and the subsequent release of inorganic**
275 **chlorine), relative to the amount of a CFC that entered at the tropopause (e.g. (Daniel et al.,**
276 **2007; Douglass et al., 2008; Laube et al., 2013; Newman et al., 2007; Schauffler et al., 2003)).**
277 **Differences in the semi-empirical vs. model ODPs in Table 6 are ,likely due, at least in part, to**
278 **differences in the observationally based fractional release factors taken for mid-latitude**
279 **conditions compared to the global model calculations. Differences in the ODPs may also arise**
280 **from differences in the Ko et al. (2013) lifetimes used for the semi-empirical ODPs vs. the model**
281 **lifetimes, although these lifetime differences are small.**

282 **4.2. Calculated Radiative Efficiencies (RE) and Global Warming Potentials (GWPs)**

283 Table 6 summarizes the radiative efficiencies (REs) for the CFCs calculated using the
284 methods described in Hodnebrog et al. (2013) and the global warming potentials (GWPs) for the
285 20, 100, and 500-year time-horizons using the lifetimes **and infrared spectra** from this work. The
286 CFCs are potent greenhouse gases and radiative forcing agents due to their high REs and long
287 atmospheric lifetimes. The GWPs for these long-lived compounds are comparable, or less than,
288 those of the atmospherically most abundant CFCs, e.g. the 100 year time-horizon GWPs for

289 CFC-11 (CCl_3F), CFC-12 (CCl_2F_2), and CFC-113 ($\text{CCl}_2\text{FCClF}_2$) are 4660, 10200, and 5820,
290 respectively (WMO, 2014). Etminan et al. (2014) reported a RE of $0.23 \text{ W m}^{-2} \text{ ppb}^{-1}$ for CFC-
291 113a and a GWP_{100} of 3310 using a lifetime of 51 years. These values are in reasonable
292 agreement with the present results.

293 5. Conclusions

294 Short wavelength UV absorption spectra for $\text{CCl}_2\text{FCCl}_2\text{F}$ (CFC-112), $\text{CCl}_3\text{CClF}_2$ (CFC-
295 112a), CCl_3CF_3 (CFC-113a), and CCl_2FCF_3 (CFC-114a) measured in this work between 192.5
296 and 235 nm and at temperatures in the range 207 to 323 K were combined with 2-D atmospheric
297 model calculations to assess their atmospheric loss processes, lifetimes, and ozone depletion
298 potentials (ODPs). Short wavelength UV photolysis was shown to be the predominant loss
299 process for the CFCs with global annually averaged lifetimes of 63.6, 51.5, 55.5, and 105.3
300 years, for CFC-112, CFC-112a, CFC-113a, and CFC-114a, respectively. The uncertainty in the
301 model-calculated lifetimes due primarily to the 2σ uncertainty in the UV absorption spectra
302 reported in this work, was found to be small, $<3\%$. These CFCs are potent ozone depleting
303 substances with 2-D model calculated ODPs of 0.98, 0.86, 0.73, and 0.72 for CFC-112, CFC-
304 112a, CFC-113a, and CFC-114a, respectively. The uncertainty in the model calculated ODPs
305 due to the uncertainty in the UV spectra and $\text{O}(^1\text{D})$ reactive loss was is small, $<\pm 0.015$. These
306 CFCs are also potent greenhouse gases with GWPs comparable to those of the most abundant
307 CFCs present in the atmosphere.

308 **Acknowledgments.** This work was supported in part by NOAA's Atmospheric Chemistry,
309 Carbon Cycle, and Climate (AC4) Program and NASA's Atmospheric Composition Program.
310 Supporting information includes digitized infrared spectra as well as additional figures, model
311 results, and tables.

312

313 **References**

- 314
- 315 Baasandorj, M., Feierabend, K. J., and Burkholder, J. B.: Rate coefficients and ClO radical yields
316 in the reaction of O(¹D) with CClF₂CCl₂F, CCl₃CF₃, CClF₂CClF₂, and CCl₂FCF₃, *Int. J.*
317 *Chem Kinet.*, 43, 1-9, doi:10.1002/kin.20561, 2011.
- 318 Burkholder, J. B., Cox, R. A., and Ravishankara, A. R.: Atmospheric degradation of ozone
319 depleting substances, their substitutes, and related species, *Chem. Rev.*, 115, 3704-3759,
320 doi:10.1021/cr5006759, 2015a.
- 321 Burkholder, J. B., Sander, S. P., Abbatt, J., Barker, J. R., Huie, R. E., Kolb, C. E., Kurylo, M. J.,
322 Orkin, V. L., Wilmouth, D. M., and Wine, P. H.: "Chemical Kinetics and Photochemical
323 Data for Use in Atmospheric Studies, Evaluation No. 18," JPL Publication 15-10, Jet
324 Propulsion Laboratory, Pasadena, 2015 <http://jpldataeval.jpl.nasa.gov/>, 2015b.
- 325 Chipperfield, M. P., Liang, Q., Strahan, S. E., Morgenstern, O., Dhomse, S. S., Abraham, N. L.,
326 Archibald, A. T., Bekki, S., Braesicke, P., Di Genova, G., Fleming, E. L., Hardiman, S.
327 C., Iachetti, D., Jackman, C. H., Kinnison, D. E., Marchand, M., Pitari, G., Pyle, J. A.,
328 Rozanov, E., Stenke, A., and Tummon, F.: Multimodel estimates of atmospheric lifetimes
329 of long-lived ozone-depleting substances: Present and future, *J. Geophys. Res.*, 119,
330 2555–2573, doi:10.1002/2013/13JD021097, 2014.
- 331 Daniel, J. S., Velders, G. J. M., Douglass, A. R., Forster, P. M. D., Hauglustaine, D. A., Isaksen,
332 I. S. A., Kuijpers, L. J. M., McCulloch, A., and Wallington, T. J.: Halocarbon scenarios,
333 ozone depletion potentials, and global warming potentials, Chapter 8 in World
334 Meteorological Organization: Scientific assessment of ozone depletion: 2006, Global
335 Ozone Research and Monitoring Project – Report No. 50, Geneva, 2007.
- 336 Douglass, A. R., Stolarski, R. S., Schoeberl, M. R., Jackman, C. H., Gupta, M. L., Newman, P.
337 A., Nielsen, J. E., and Fleming, E. L.: Relationship of loss, mean age of air and the
338 distribution of CFCs to stratospheric circulation and implications for atmospheric
339 lifetimes, *J. Geophys. Res.*, 113, D14309, doi:10.1029/2007JD009575, 2008.
- 340 Etminan, M., Highwood, E. J., Laube, J. C., McPheat, R., Marston, G., Shine, K. P., and Smith,
341 K. M.: Infrared absorption spectra, radiative efficiencies, and global warming potentials
342 of newly-detected halogenated compounds: CFC-113a, CFC-112 and HCFC-133a,
343 *Atmosphere*, 5, 473-483, doi:10.3390/atmos5030473, 2014.
- 344 Fisher, D. A., Hales, C. H., Filkin, D. L., Ko, M. K. W., Sze, N. D., Connell, P. S., Wuebbles, D.
345 J., Isaksen, I. S. A., and Stordal, F.: Model calculations of the relative effects of CFCs
346 and their replacements on stratospheric ozone, *Nature*, 344, 508–512,
347 doi:10.1038/344513a0, 1990.
- 348 Fleming, E. L., Jackman, C. H., Stolarski, R. S., and Douglas, A. R.: A model study of the
349 impact of source gas changes on the stratosphere for 1850-2100, *Atmos. Chem. Phys.*,
350 11, 8515-8541, doi:10.5194/acp-11-8515-2011, 2011.
- 351 Hodnebrog, Ø., Etminan, M., Fuglestvedt, J. S., Marston, G., Myhre, G., Nielsen, C. J., Shine, K.
352 P., and Wallington, T. J.: Global warming potentials and radiative efficiencies of
353 halocarbons and related compounds: A comprehensive review, *Rev. Geophys.*, 51, 300–
354 378, doi:10.1002/rog.20013, 2013.
- 355 Lifetimes of Stratospheric Ozone-Depleting Substances, Their Replacements, and Related
356 Species, 2013.
- 357 Laube, J. C., Keil, A., Bönisch, H., Engel, A., Röckmann, T., Volk, C. M., and Sturges, W. T.:
358 Observation-based assessment of stratospheric fractional release, lifetimes, and ozone

359 depletion potentials of ten important source gases *Atmos. Chem. Phys.*, 13, 2779–2791,
360 doi:10.5194/acp-13-2779-2013 2013.

361 Laube, J. C., Newland, M. J., Hogan, C., Brenninkmeijer, C. A. M., Fraser, P. J., Martinerie, P.,
362 Oram, D. E., Reeves, C. E., Röckmann, T., Schwander, J., Witrant, E., and Sturges, W.
363 T.: Newly detected ozone-depleting substances in the atmosphere, *Nature Geoscience*, 7,
364 266–269, doi:10.1038/ngeo2109, 2014.

365 McGillen, M. R., Fleming, E. L., Jackman, C. H., and Burkholder, J. B.: CFC₁₁ (CFC-11): UV
366 absorption spectrum temperature dependence measurements and the impact on its
367 atmospheric lifetime and uncertainty, *Geophys. Res. Lett.*, 40, 4772–4776,
368 doi:10.1002/grl.50915, 2013.

369 Newman, P. A., Daniel, J. S., Waugh, D. W., and Nash, E. R.: A new formulation of equivalent
370 effective stratospheric chlorine (EESC), *Atmos. Chem. Phys.*, 7, 4537–4552,
371 doi:10.5194/acp-7-4537-2007, 2007.

372 Olliff, M., and Fischer, G.: Integrated band intensities of 1,1,1-trichlorotrifluoroethane,
373 CFC113a, and 1,1,2-trichlorotrifluoroethane, CFC113, *Spectrochimica Acta Part a-*
374 *Molecular and Biomolecular Spectroscopy*, 48, 229–235, doi:10.1016/0584-
375 8539(92)80028-u, 1992.

376 Olliff, M. P., and Fischer, G.: Integrated absorption intensities of haloethanes and halopropanes,
377 *Spectrochimica Acta Part a-Molecular and Biomolecular Spectroscopy*, 50, 2223–2237,
378 doi:10.1016/0584-8539(93)e0027-t, 1994.

379 Papadimitriou, V. C., McGillen, M. R., Fleming, E. L., Jackman, C. H., and Burkholder, J. B.:
380 NF₃: UV absorption spectrum temperature dependence and the atmospheric and climate
381 forcing implications, *Geophys. Res. Lett.*, 40, 1–6, doi:10.1002/grl.50120, 2013a.

382 Papadimitriou, V. C., McGillen, M. R., Smith, S. C., Jubb, A. M., Portmann, R. W., Hall, B. D.,
383 Fleming, E. L., Jackman, C. H., and Burkholder, J. B.: 1,2-Dichlorohexafluoro-
384 cyclobutane (1,2-c-C₄F₆Cl₂, R-316c) a potent ozone depleting substance and greenhouse
385 gas: Atmospheric loss processes, lifetimes, and ozone depletion and global warming
386 potentials for the (*E*) and (*Z*) stereoisomers, *J. Phys. Chem. A*, 117, 11049–11065,
387 doi:10.1021/jp407823k, 2013b.

388 Plumb, R. A., and Ko, M. K. W.: Interrelationships between mixing ratios of long-lived
389 stratospheric constituents, *J. Geophys. Res.*, 97, 10140–10156, doi:10.1029/92JD00450,
390 1992.

391 Sander, S. P., Abbatt, J., Barker, J. R., Burkholder, J. B., Friedl, R. R., Golden, D. M., Huie, R.
392 E., Kolb, C. E., Kurylo, M. J., Moortgat, G. K., Orkin, V. L., and Wine, P. H.: Chemical
393 Kinetics and Photochemical Data for Use in Atmospheric Studies, Evaluation Number
394 17, 2011, <http://jpldataeval.jpl.nasa.gov/>.

395 Schauffler, S. M., Atlas, E. L., Donnelly, S. G., Andrews, A., Montzka, S. A., Elkins, J. W.,
396 Hurst, D. F., Romashkin, P. A., Dutton, G. S., and Stroud, V.: Chlorine budget and
397 partitioning during SOLVE, *J. Geophys. Res.*, 108, 4173, doi:10.1029/2001JD002040,
398 2003.

399 Volk, C. M., Elkins, J. W., Fahey, D. W., Dutton, D. S., Gilligan, J. M., Loewenstein, M.,
400 Podolske, J. R., Chan, K. R., and Gunson, M. R.: Evaluation of source gas lifetimes from
401 stratospheric observations, *J. Geophys. Res.*, 102, 25543–25564, doi:10.1029/97JD02215,
402 1997.

403 WMO (World Meteorological Organization), Scientific Assessment of Ozone Depletion: 2014,
404 Global Ozone Research and Monitoring Project-Report No. 55, 416 pp., Geneva,
405 Switzerland, 2014.

406 Wuebbles, D. J.: Chlorocarbon emission scenarios: potential impact on stratospheric ozone,
407 Geophys. Res. Lett., 88, 1433-1443, doi:10.1029/JC88iC02p01433, 1983.

408

409

410 **Table 1.** CCl₃CF₃ (CFC-113a) UV Absorption Cross Section Data (10⁻²⁰ cm² molecule⁻¹, base e)
 411 Obtained in This Work.

λ (nm)	323 K	296 K	271 K	250 K	232 K	207 K
192.5	131.6 ± 1.5	132.5 ± 1.1	136.9 ± 1.0	137.2 ± 0.9	141.4 ± 1.6	139.7 ± 0.9
195	103.9 ± 0.2	106.6 ± 0.6	106.8 ± 0.9	107.5 ± 1.2	110.2 ± 1.0	111.0 ± 0.3
200	64.3 ± 0.2	63.9 ± 0.6	63.9 ± 1.2	63.6 ± 0.6	64.5 ± 0.6	63.5 ± 0.4
205	35.3 ± 0.14	34.1 ± 0.2	33.5 ± 0.13	33.2 ± 0.2	31.9 ± 0.3	31.3 ± 0.3
210	17.3 ± 0.10	16.2 ± 0.1	15.3 ± 0.1	14.4 ± 0.1	13.9 ± 0.17	12.5 ± 0.2
215	7.99 ± 0.02	7.25 ± 0.01	6.58 ± 0.02	5.94 ± 0.06	5.77 ± 0.06	5.26 ± 0.07
220	3.57 ± 0.014	3.07 ± 0.02	2.65 ± 0.007	2.36 ± 0.02	2.23 ± 0.008	2.09 ± 0.02
225	1.55 ± 0.014	1.29 ± 0.01	1.04 ± 0.004	0.912 ± 0.006	0.813 ± 0.01	0.778 ± 0.04
230	0.673 ± 0.009	0.521 ± 0.004	0.418 ± 0.003	0.357 ± 0.008	0.322 ± 0.003	
235	0.297 ± 0.018	0.208 ± 0.001	0.157 ± 0.006	0.139 ± 0.006		

412 * Quoted uncertainties are 2σ fit precision values (rounded off).

413

414

415 **Table 2.** CCl₂FCF₃ (CFC-114a) UV Absorption Cross Section Data (10⁻²⁰ cm² molecule⁻¹, base
 416 e) Obtained in This Work.

λ (nm)	323 K	296 K	271 K	250 K	232 K	207 K
192.5	32.8 ± 0.2	32.2 ± 0.3	31.6 ± 0.2	30.7 ± 0.2	30.0 ± 0.3	28.2 ± 0.2
195	21.8 ± 0.1	20.7 ± 0.1	19.9 ± 0.1	19.0 ± 0.1	18.4 ± 0.1	17.3 ± 0.1
200	8.72 ± 0.01	7.86 ± 0.045	7.26 ± 0.02	6.70 ± 0.03	6.26 ± 0.04	5.88 ± 0.05
205	3.31 ± 0.01	2.86 ± 0.01	2.50 ± 0.03	2.29 ± 0.02	2.12 ± 0.02	1.91 ± 0.02
210	1.21 ± 0.003	0.991 ± 0.003	0.835 ± 0.006	0.757 ± 0.006	0.655 ± 0.083	0.555 ± 0.002
215	0.440 ± 0.002	0.345 ± 0.001	0.276 ± 0.001	0.246 ± 0.006	0.197 ± 0.001	0.168 ± 0.001
220	0.162 ± 0.002	0.118 ± 0.0004	0.0926 ± 0.0003	0.0786 ± 0.0013	0.0626 ± 0.0003	0.0534 ± 0.0014
225	0.0600 ± 0.001	0.0409 ± 0.0006	0.0307 ± 0.0002	0.0253 ± 0.0002	0.0204 ± 0.0004	0.0176 ± 0.0046
230		0.0147 ± 0.0004	0.0110 ± 0.0002			
235		0.00553 ± 0.00025				

417 * Quoted uncertainties are 2 σ fit precision values (rounded off).

418

419

420

421 **Table 3.** Parameterization of the UV absorption spectra for CCl₂FCCl₂F (CFC-112), CCl₃CClF₂
 422 (CFC-112a), CCl₃CF₃ (CFC-113a), and CCl₂FCF₃ (CFC-114a) obtained in this work. The
 423 parameterization is for wavelengths between 192.5 to 235 nm and temperatures between 230 and
 424 323 K for CFC-112 and CFC-112a and between 207 and 323 K for CFC-113a and CFC-114a.
 425 Units: $\sigma(\lambda, T)$ (cm² molecule⁻¹, base e), λ (nm), and T (K)

$$426 \quad \ln(\sigma(\lambda, T)) = \sum_i A_i \lambda_i^i + (T - 296) \sum_i B_i \lambda_i^i$$

Molecule	<i>i</i>	<i>A_i</i>	<i>B_i</i>
CCl ₂ FCCl ₂ F (CFC-112)	0	-1488.6207	6.04688
	1	18.43604	-0.0801501
	2	-0.02897393	0.0001201698
	3	-0.00051504703	2.610366 × 10 ⁻⁶
	4	2.644261 × 10 ⁻⁶	-1.3959106 × 10 ⁻⁸
	5	-3.7258313 × 10 ⁻⁹	2.0719264 × 10 ⁻¹¹
CCl ₃ CClF ₂ (CFC-112a)	0	-560.3404	10.37492
	1	9.534427	-0.182485408
	2	-0.06987945	0.0011614979
	3	0.0002657157	-2.9864183 × 10 ⁻⁶
	4	-5.491224 × 10 ⁻⁷	1.547878 × 10 ⁻⁹
	5	4.993769 × 10 ⁻¹⁰	3.36518 × 10 ⁻¹²
CCl ₃ CF ₃ (CFC-113a)	0	-319.173	2.89174
	1	2.70954	-0.0348043
	2	0.00457404	3.6233 × 10 ⁻⁵
	3	-0.0001288147	1.08853 × 10 ⁻⁶
	4	4.71409 × 10 ⁻⁷	-5.25744 × 10 ⁻⁹
	5	-5.35388 × 10 ⁻¹⁰	7.26095 × 10 ⁻¹²
CCl ₂ FCF ₃ (CFC-114a)	0	-253.6338	0.52031
	1	2.899454	-0.005044
	2	-0.0081158	1.6142 × 10 ⁻⁶
	3	-3.68328 × 10 ⁻⁵	7.2259 × 10 ⁻⁸
	4	2.071842 × 10 ⁻⁷	2.4996 × 10 ⁻¹¹
	5	-2.5764 × 10 ⁻¹⁰	-5.9642 × 10 ⁻¹³

427

428

429

430 **Table 4.** Fractional losses and ranges (in parenthesis) for CCl₂FCCl₂F (CFC-112), CCl₃CClF₂
 431 (CFC-112a), CCl₃CF₃ (CFC-113a), and CCl₂FCF₃ (CFC-114a) calculated using the GSFC 2-D
 432 model and the UV absorption spectra and estimated Lyman- α cross sections reported in this
 433 work

Molecule	Lyman- α	190-230 nm	O(¹ D)
CCl ₂ FCCl ₂ F (CFC-112)	<0.001	0.978 (0.953–0.99)	0.022 (0.047–0.01)
CCl ₃ CClF ₂ (CFC-112a)	<0.001	0.979 (0.955–0.99)	0.021 (0.045–0.01)
CCl ₃ CF ₃ (CFC-113a)	<0.001	0.979 (0.968–0.986)	0.021 (0.032–0.014)
CCl ₂ FCF ₃ (CFC-114a)	<0.001	0.929 (0.903–0.948)	0.071 (0.097–0.052)

434

435

436

437

438

439 **Table 5.** Atmospheric lifetimes (τ)^a and ranges^b (years) for CCl₂FCCl₂F (CFC-112), CCl₃CClF₂
 440 (CFC-112a), CCl₃CF₃ (CFC-113a), and CCl₂FCF₃ (CFC-114a) calculated using the GSFC 2-D
 441 model and the UV absorption spectra reported in this work

Molecule	Tropospheric		Stratospheric		Mesospheric	Total	
	τ	τ Range	τ	τ Range	τ	τ	τ Range
CCl ₂ FCCl ₂ F (CFC-112)	2276	(1718–2710)	65.4	(64.2–66.3)	>10 ⁶	63.6	(61.9–64.7)
CCl ₃ CClF ₂ (CFC-112a)	1187	(938–1371)	53.8	(52.8–54.6)	>10 ⁶	51.5	(50.0–52.6)
CCl ₃ CF ₃ (CFC-113a)	1476	(1290–1645)	57.5	(56.7–58.3)	>10 ⁶	55.4	(54.3–56.3)
CCl ₂ FCF ₃ (CFC-114a)	8312	(6286–10480)	106.7	(104.7–108.6)	3 × 10 ⁵	105.3	(102.9–107.4)

442 ^a Global annually averaged values; ^b Calculated using 2 σ upper and lower limits of the UV
 443 absorption cross sections and estimated Lyman- α cross sections reported in this work (see text)
 444 and O(¹D) rate coefficient uncertainties from Sander et al. (2011).

445

446

447
448
449

Table 6. Lifetimes, ozone depletion potentials (ODPs), radiative efficiencies (RE), and global warming potentials (GWPs) obtained in this work and literature values for comparison

Molecule	Lifetime (years)	Ozone Depletion Potential (ODP)		Radiative Efficiency ($\text{W m}^{-2} \text{ppb}^{-1}$)	Global Warming Potential Time Horizons (years)		
		semi-empirical	2-D Model ^d		20	100	500
CCl ₂ FCCl ₂ F (CFC-112)	63.6	0.88 (0.62-1.44) ^a	0.98 (± 0.015)	0.28	5330	4260	1530
CCl ₃ CClF ₂ (CFC-112a)	51.5	0.88 (0.50-2.19) ^a	0.86 (± 0.015)	0.25	4600	3330	1110
CCl ₃ CF ₃ (CFC-113a)	55.4	0.68 (0.34-3.79) ^a	0.73 (± 0.01)	0.24	4860	3650	1240
CCl ₂ FCF ₃ (CFC-114a)	105.3		0.72 (± 0.01)	0.28	6750	6510	3000
CCl ₂ FCClF ₂ (CFC-113)	93 ^b	0.81-0.82 ^b	0.95	0.30 ^b	6490 ^b	5820 ^b	
CClF ₂ CClF ₂ (CFC-114)	189 ^b	0.50 ^b	0.78	0.31 ^b	7710 ^b	8590 ^b	
CClF ₂ CF ₃ (CFC-115)	540 ^b	0.26 ^b	0.44	0.20 ^b	5860 ^b	7670 ^b	
CCl ₃ F ₂ (CFC-12)	102 ^b	0.73-0.81 ^b	1.01	0.32 ^b	10800 ^b	10200 ^b	
CCl ₄	26 ^{b,c}	0.72 ^b	1.06	0.17 ^b	3480 ^b	1730 ^b	

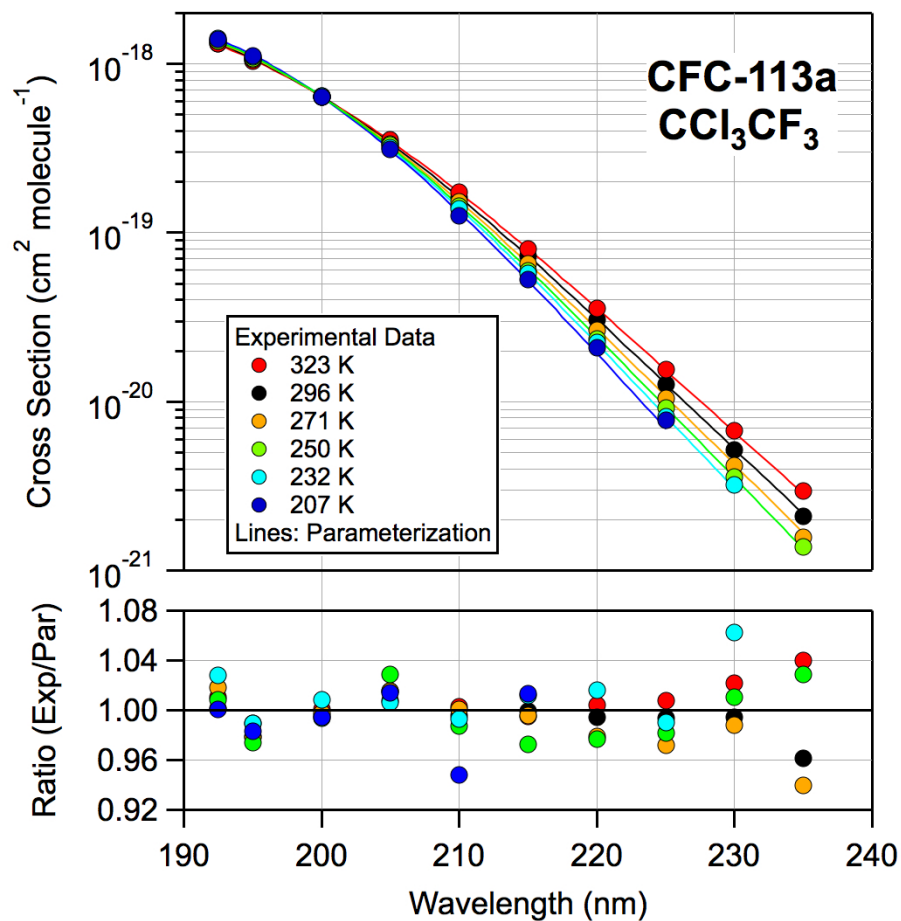
450
451
452
453
454
455
456
457

^a Semi-empirical ODPs and uncertainty ranges taken from Laube et al. (2014).

^b Taken from WMO (2014).

^c CCl₄ stratospheric lifetime of 44 years given in WMO (2014).

^d The uncertainty range in the model calculated ODPs reported here is due solely to the uncertainty in the UV and Lyman- α (estimated) spectra obtained in this work and uncertainty in the O(¹D) rate coefficients taken from Sander et al. (2011).

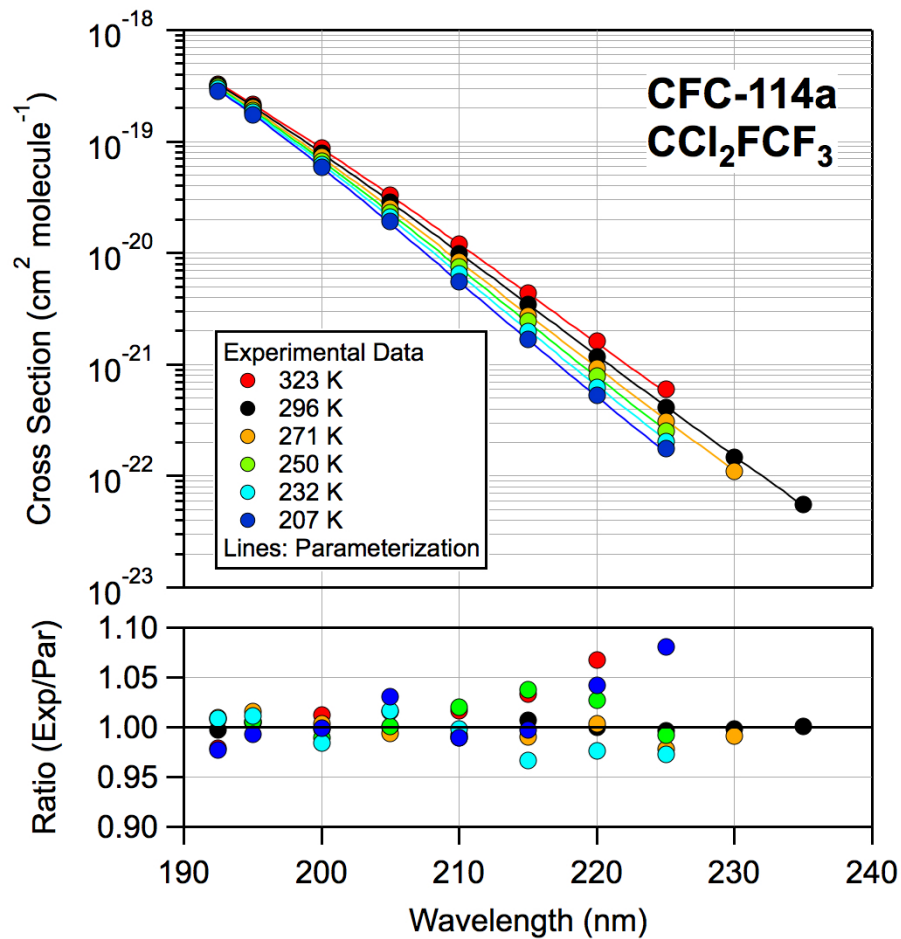


459

460 **Figure 1.** CCl_3CF_3 (CFC-113a) UV absorption spectrum (base e) and parameterization obtained
 461 in this work. Cross section data (symbols, Table 1) and the parameterization of the data using
 462 the empirical formula and parameters given in Table 3 (see text). The lower frame shows the
 463 overall quality of the parameterization.

464

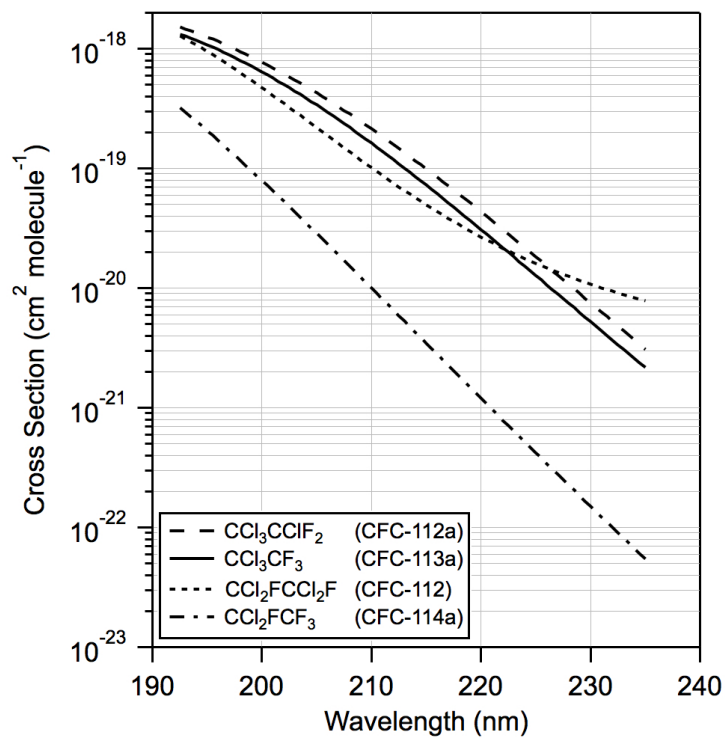
465
466



467
468
469
470
471
472
473
474

Figure 2. CCl_2FCF_3 (CFC-114a) UV absorption spectrum (base e) and parameterization obtained in this work. Cross section data (symbols, Table 2) and the parameterization of the data using the empirical formula and parameters given in Table 3 (see text). The lower frame shows the overall quality of the parameterization.

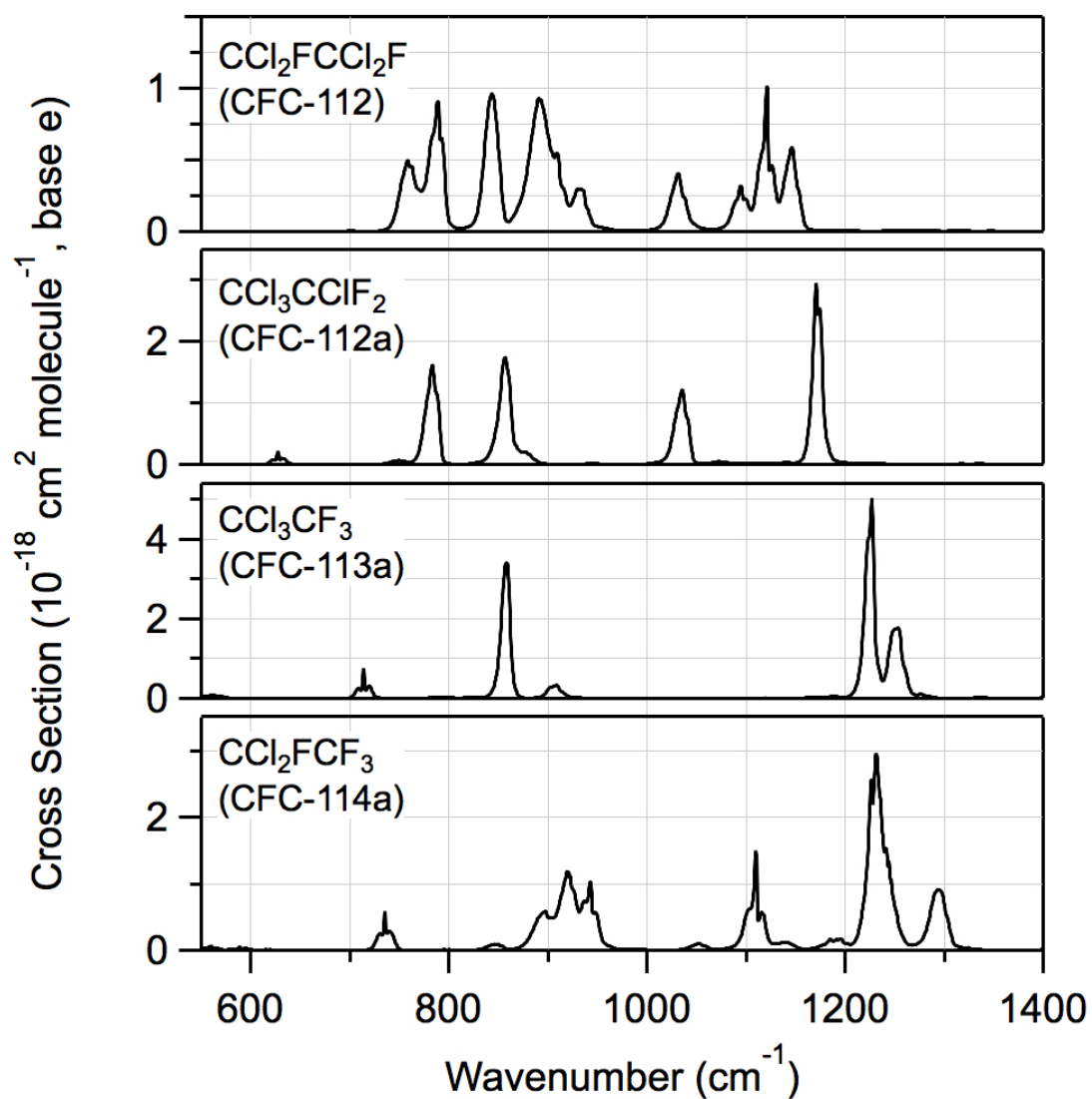
475
476



477
478 **Figure 3.** UV absorption spectra (base e) of CFC-112, CFC-112a, CFC-113a, and CFC-114a at
479 296 K calculated using the parameterization from this work, Table 3, over the wavelength range
480 of our experimental measurements.

481
482

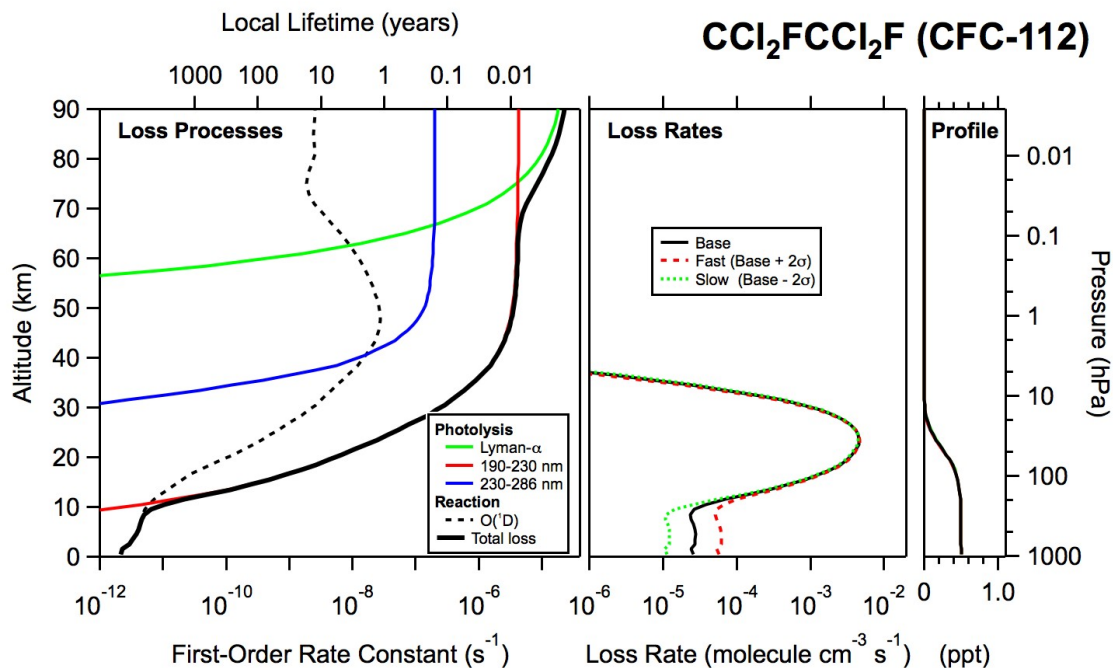
483
484



485
486
487
488
489
490
491

Figure 4. Infrared absorption spectra of $\text{CCl}_2\text{FCCl}_2\text{F}$ (CFC-112), $\text{CCl}_3\text{CClF}_2$ (CFC-112a), CCl_3CF_3 (CFC-113a), and CCl_2FCF_3 (CFC-114a) at 296 K obtained in this work.

492
493



494
495
496
497
498
499
500
501
502
503

Figure 5. Global annually averaged vertical profiles of the atmospheric loss processes, molecular loss rates, and mixing ratio for $\text{CCl}_2\text{FCCl}_2\text{F}$ (CFC-112) calculated using the GSFC 2-D atmospheric model for year 2000. The model calculations were performed using the CFC-112 UV absorption spectrum from this work and other model input parameters taken from the literature as described in the text. The global annually averaged lifetime for CFC-112 was calculated to be 63.6 (61.9–64.7) years.